Time-Resolved Step-Scan Fourier Transform Infrared Spectroscopy Reveals Differences between Early and Late M Intermediates of Bacteriorhodopsin

C. Rödig,* I. Chizhov,# O. Weidlich,* and F. Siebert*

*Institut für Biophysik und Strahlenbiologie der Universität Freiburg, 79104 Freiburg, and #Max-Planck-Institut für Molekulare Physiologie, 44139 Dortmund, Germany

ABSTRACT In this report, from time-resolved step-scan Fourier transform infrared investigations from 15 ns to 160 ms, we provide evidence for the subsequent rise of three different M states that differ in their structures. The first state rises with ~3 μs to only a small percentage. Its structure as judged from amide I/II bands differs in small but well-defined aspects from the L state. The next M state, which appears in ~40 μs, has almost all of the characteristics of the "late" M state, i.e., it differs considerably from the first one. Here, the L ↔ M equilibrium is shifted toward M, although some percentage of L still persists. In the last M state (rise time ~130 μs), the equilibrium is shifted toward full deprotonation of the Schiff base, and only small additional structural changes take place. In addition to these results obtained for unbuffered conditions or at pH 7, experiments performed at lower and higher pH are presented. These results are discussed in terms of the molecular changes postulated to occur in the M intermediate to allow the shift of the L/M equilibrium toward M and possibly to regulate the change of the accessibility of the Schiff base necessary for effective proton pumping.

INTRODUCTION

All models of the mechanism of the light-driven proton pump bacteriorhodopsin (BR) assume that it is the proton of the protonated Schiff base through which the chromophore all-*trans* retinal is bound to Lys^{216}, which is being pumped (Haupts et al., 1997; Spudich and Lanyi, 1996; Brown et al., 1998). Light absorption isomerizes the chromophore to a distorted 13-*cis* geometry, and this primary molecular event is followed by thermal relaxations of the chromophore and the protein, resulting in pK_a well adjusted changes in time of the Schiff base and the primary proton acceptor and donor Asp^{85} and Asp^{96}, respectively. This allows proton transfer from the Schiff base to Asp^{85} and, at a later stage, reprotonation of the Schiff base from Asp^{96} (see Mathies et al., 1991; Rothschild, 1992; Oesterhelt et al., 1992; Ebrey, 1993; Lanyi, 1993, for reviews on BR). In the same time range as that in which the proton is transferred from the Schiff base to Asp^{85} and apparently triggered by this process, a proton appears at the extracellular surface. For this, additional pK_a changes have to take place, and evidence has been provided that Glu^{204}, Glu^{194}, and probably Arg^{82} are involved (Balashov et al., 1995, 1996; Misra et al., 1997; Brown et al., 1995; Richter et al., 1996a,b; Dioumaev et al., 1998), although there is some debate about the precise role of these amino acids (Rammelsberg et al., 1998).

Irrespective of these details, there has to be a mechanism that inhibits, after the pK_a of the deprotonated Schiff base is increased for its reprotonation, the proton uptake from the same side to which it has been ejected. This has led to the concept of accessibility change of the Schiff base: in the first phase, it has to be connected to Asp^{85} and the extracellular side, and in the second phase the connection has to be to Asp^{96} and the cytosolic side. This can be achieved by appropriate pK_a changes of groups involved in proton transport (Honig, 1978) and/or by real geometrical alterations, allowing for reprotonation of the Schiff base only from the cytosolic side. Thus corresponding structural changes have to occur (termed "molecular switch") that regulate these processes. Therefore two M states were claimed: in M1 the connectivity of the Schiff base is still to the extracellular side, whereas in M2 it is toward the cytosolic side (Ames and Mathies, 1990; Váró and Lanyi, 1991b; Kataoka et al., 1994; Tittor et al., 1994). In addition to the molecular changes regulating the accessibility of the Schiff base, there are molecular processes that may be either directly correlated or rather independent, which control the deprotonation of the Schiff base by adjusting the pK_a's of the Schiff base and Asp^{85} (Braiman et al., 1996; Brown et al., 1993; Brown and Lanyi, 1996). An early M has been identified that is in equilibrium with L, the equilibrium constant favoring L, whereas for the late M state(s), the equilibrium is shifted, depending on the pH, to more or less full deprotonation of the Schiff base (Váró and Lanyi, 1990; Chizhov et al., 1996).

Recently, a mechanism has been proposed that increases the pK_a of the proton acceptor Asp^{85} during the rise of M and shifts the L ↔ M equilibrium to full deprotonation of the Schiff base. Above pH 5.4, protonation of Asp^{85} initiates the proton release from the interface region of the extracellular side of the membrane, probably involving the residues Arg^{82}, Glu^{204}, and Glu^{194}. This in turn rises the pK_a of Asp^{85}. The interaction mediating the pK_a changes is

Received for publication 26 August 1998 and in final form 28 December 1998.

Address reprint requests to Dr. F. Siebert, Institut für Biophysik und Strahlenbiologie der Universität Freiburg, Albertstrasse 23, 79104 Freiburg i. Br., Germany. Tel.: +49-761-2035396; Fax: +49-761-2035399 or 2035016; E-mail: frisi@ruf.uni-freiburg.de.

0006-3495/99/05/2687/15 $2.00

thought to be mainly electroststic. Below pH 5.4, the proton is not released and the L ↔ M equilibrium persists throughout the lifetime of M (Balashov et al., 1995, 1996; Misra et al., 1997; Brown et al., 1995; Richter et al., 1996a,b; Dioumaev et al., 1998). From time-resolved resonance Raman experiments measuring the pH dependence of the L ↔ M equilibrium, it has been concluded that additional factors such as protein conformational changes must be involved to regulate the pK_a values (Althaus and Stockburger, 1998).

Experimental evidence for the existence of different M states has come from kinetic analysis of the photocycle (Váró and Lanyi, 1991b), from kinetic and spectral studies of mutants (Váró et al., 1992; Zimányi et al., 1992a; Cao et al., 1995), from kinetic and spectral analysis of the light-induced back-reaction from the M states (Druckmann et al., 1992; Hessling et al., 1997), and from the analysis of the corresponding photocurrents (Dickopf and Heyn, 1997). In addition, an M state has been described, the lifetime of which is considerably prolonged by the application of an electric field opposite the proton movement, and it has been demonstrated that in this state the connectivity is still to the extracellular side (Nagel et al., 1998). Therefore, it has the properties of M1. However, from all of these investigations it has not yet been possible to identify clear structural differences between the different M states. Further evidence for a heterogeneous M population with states differing in protein conformations has come from low-temperature spectroscopy in combination with blue-light back-reaction (Friedman et al., 1994).

To detect molecular changes taking place during the lifetime of the M intermediate of BR, we applied time-resolved step-scan Fourier transform infrared (FTIR) difference spectroscopy to measure the BR photocycle at different pH values in the time range from 15 ns to 160 ms. Analysis of the data with two different procedures yielded essentially identical results: for the first approach global multiexponential fitting was used, from which intermediate spectra were calculated; the second method is based on the determination of L → M difference spectra corrected for contributions of other intermediates by spectral criteria.

MATERIALS AND METHODS

For the infrared measurements, well-hydrated BR film samples have been used (Weidlich et al., 1995). For this, ~140 μg BR was dried onto a BaF_2 window, resulting in a circular film area of 1 cm^2. The film was rehydrated with 0.5 μl H_2O and sealed with a second BaF2 window. Time-resolved tests in the UV-vis showed photcycle kinetics typical of BR in excess water. Experiments have been performed either at fixed pH, using 500 nmol phosphate or borate buffer, or without buffer at a temperature of 298 K. Spectral resolution for all step-scan FTIR measurements was 8 cm^{-1}.

To cover the time range from 10 ns to the end of the photocycle, two separate measurements have been performed with our instrument (Uhmann et al., 1991; Weidlich and Siebert, 1993), which was modified for higher time resolution. This was necessary because the total time of data acquisition by the transient recorder board (200-MHz sampling rate, 8-bit resolution, model PAD-82; Spectrum, Germany) is limited by its memory of 256 K to 1.2 ms. In the first measurement, the fast detection system equipped with a fast photovoltaic MCT detector (Kolmar Technologies type KV 104–1 and appropriate dc-coupled preamplifier) was employed. The signal from the preamplifier was further amplified by 40 dB, using a fast dc-coupled, switchable dc-compensating amplifier, modified from the previous version (Weidlich and Siebert, 1993) for higher time resolution (Rödig and Siebert, 1998). This allows the simultaneous recording of the dc value and of the time-dependent change of the interferogram at each mirror position, facilitating the calculation of the spectra (Uhmann et al., 1991). The effective rise time was 40 ns, and a time range up to 160 μs was covered. The spectra shown consist of an average of nine separate measurements with 16 flashes each at every mirror position. For the slow measurements, covering the time range from 200 ns to 160 ms, a photoconductive MCT detector (Judson) with appropriate dc-coupled preamplifier and two separate transient recorder boards (PAD82 and PAD52) have been used, one operating with a sampling rate of 100 ns, the other with one of 10 kHz. The signal was further amplified by a dc-coupled, switchable dc-compensating main amplifier. The effective rise time was 500 ns in this case. For the PAD52, the electronic bandwidth was reduced according to the smaller sampling rates. For the data shown, four separate measurements were averaged with eight flashes each at every mirror position. Thus, as a consequence of the reduced electronic bandwidth, the total measuring time is reduced by a factor of ~4 as compared to the fast measurement. The method of calculating the time-resolved difference spectra from the time-resolved data has been described (Uhmann et al., 1991). To reduce the amount of data, the linear time scale was converted to a quasilogarithmic one, averaging over an increasing number of data points (Austin et al., 1976). The number of linearly spaced data points in one sector is eight, and the spacing doubles from one sector to the next.

For the global fit of the time-resolved spectra to a sum of exponentials, the program developed by Müller and Plesser (1991) has been used. Because in the time range of 1 ms and longer the data exhibit some systematic noise, only the wavenumber dependence of the statistical weights has been taken into account. The origin of the systematic noise will be treated elsewhere.

Strategy for obtaining spectra characterizing the transitions to the different M states

There are several factors that make it difficult to detect differences between the various M states: 1. According to the analysis of time-resolved UV-vis measurements, the amplitude of the early M state is very small because the L/M equilibrium favors the L state, whereas the main M amplitude develops in the transition to the late M state (Váró and Lanyi, 1991b). 2. A similar analysis of the UV-vis data indicates the existence of an KL/L equilibrium (Váró and Lanyi, 1991a). Thus the KL state may contribute to the difference spectra during the lifetime of the early L/M equilibrium. 3. Because in unmodified BR there appears to be no spectral differences in the UV-vis between the different M states (Váró and Lanyi, 1991b), it is most likely that the spectral differences monitored in the infrared will be small and restricted to changes in the protein. The expected small differences make it questionable to directly obtain information on the structural differences of the M states from the amplitude spectra of global-fit procedures. To circumvent these difficulties, two different strategies were developed that essentially yield the same results.

Procedure I

A global-fit procedure was applied to the time-resolved difference spectra. The corresponding amplitude spectra were analyzed according to the method suggested by Chizhov et al. (1996), in which a unidirectional reaction model describing transitions between unresolved fast equilibria of pure states is assumed, and the analysis yields the difference spectra to these equilibria, for which the parent state is always nonilluminated BR. In the corresponding analysis of time-resolved UV-vis data, pure KL and L states were obtained, whereas three M states were described that differ in the relative admixture of L: in the first state the equilibrium favors L, in the later state a large shift of the equilibrium toward M takes place, and the

third state represents an almost pure M state (Chizhov et al., 1996). If now in the corresponding analysis of the infrared spectra the pure L difference spectrum is subtracted from the spectra corresponding to the L/M mixtures, spectra are obtained that reflect the molecular changes of the L → M transition. Here it is assumed that no changes occur in the L intermediate. Spectral changes between the early and late M states then should be reflected in the three difference spectra of the early, intermediate, and late L → M transition. The adoption of the unidirectional reaction model for the analysis of the time-resolved spectra does not mean that we claim this model represents the true path of the photocycle. It only provides more a direct means of describing the molecular events than the amplitude spectra of the global fit themselves. The latter are strongly influenced by the kinetic constants and therefore are much more difficult to interpret. Moreover, this model does not suffer from the problem of free parameters, i.e., it allows the gathering of valuable spectral information of the processes via algebraic deconvolution of the global fit results.

In principle, the spectral differences of the M states derived in this way could also be attributed to different L states. In the Results we will provide arguments against this interpretation. However, taking the model of Chizhov et al. in its original sense renders the discrimination between differences ocurring in the L or M states unnecessary. Here transitions between protein states are described, which in turn determine the equilibria of chromophore states (L/M). It is important to note that as for structurally different M states, the protein states could represent the structural changes related to the shift in protonation equilibrium and changes in the accessibility of the Schiff base. These considerations also apply to procedure II, another approach to unraveling different M states from the time-resolved spectra.

Procedure II

1. The content of the KL state in the early (microsecond) difference spectra was taken into account by subtracting an appropriate percentage of a BR → KL difference spectrum. This yields BR → L/M difference spectra with varying relative contents of L, early, and late M. The criteria for correct subtraction of the BR → KL difference spectrum and selection of the appropriate KL spectrum will be described in the Results. Taking the subtraction constant into account, the resulting spectra are normalized to equal BR turnover.

2. The earliest microsecond spectrum, essentially containing L, is subtracted from all of the later spectra. Because the spectra have been normalized, the fingerprint bands of the chromophore of the BR state (between 1260 and 1160 cm^{-1}) are canceled. Thus L → M difference spectra are obtained with varying relative amounts of the different M states. Again, it is assumed that the L intermediate does not undergo spectral changes.

3. To compensate for the different degree of turnover (i.e., in the early spectra less L has transformed to the M states as compared to the later spectra), the spectra are normalized to each other; the criteria for this are given in the Results.

If there are no differences between the early L → M spectra and the later ones, we also have to conclude that infrared spectroscopy is not sensitive to the molecular differences between the M states. However, any consistent spectral differences increasing with time can be taken as resulting from the molecular changes between the different M states.

RESULTS

Fig. 1 *A* shows selected step-scan FTIR difference spectra of the photoreaction of bacteriorhodopsin at pH 7 up to 460 ns, using the fast detection system. For a better comparison, the spectra have been normalized to the depletion bands of BR, thereby correcting for the effective instrumental rise time of ~40 ns. The time slices shown here as resulting from the quasilogarithmic time base are 15, 25, 80, 200, and 460 ns. With the exception of a few features discussed later, the spectra are in good agreement with recently published step-scan FTIR difference spectra (Hage et al., 1996; Dioumaev and Braiman, 1997). We agree in particular with the conclusions derived by Dioumaev and Braiman (1997) that there exist two KL states that mainly differ in the intensity of the hydrogen-out-of-plane (HOOP) mode at 957 cm^{-1}, whereas the HOOP mode at 983 cm^{-1}, which has been assigned to the 15-H HOOP vibration based on isotopic substitution (Weidlich and Siebert, 1993), remains almost unchanged in the two states. Furthermore, the intensity of the fingerprint band at 1190 cm^{-1} is reduced. The transition time is shorter than 100 ns at 300 K (Dioumaev and Braiman, 1997) and is not clearly resolved in these measurements. Thus to correct for KL contributions in the microsecond spectra according to procedure II, the late KL spectrum must be used. The comparison of our directly measured spectra with the pure spectra derived by kinetic analysis (Dioumaev and Braiman, 1997) shows that the spectra of the 300-ns time range represent an appropriate approximation with still very little L present. Any contribution of the L state, which has already appeared to a small extent, does not affect the basis of this method. It only reduces the L amplitude in the resulting BR → L/M difference spectra but does not influence the evaluation of the L → M difference spectra.

Fig. 1 *B* shows the spectra in the 1.9 to 280 μs time range, using the slower detection system and, in addition, the last spectrum of Fig. 1 *A* (*top spectrum*). The measurement covers the time range up to maximum M formation. The time slices resulting from the quasilogarithmic time base are 1.9, 4.8, 10, 15, 24, 75, 170, and 280 μs. In the spectra up to 4.8 μs, the positive band at 1512 cm^{-1} indicates the presence of the KL state. The last two spectra exhibit all of the characteristics of the BR → M (actually late M) transition, i.e., protonation of Asp^{85} (positive band at 1761 cm^{-1}, characteristic amide I bands, the positive band around 1554 cm^{-1}, mainly due to amide II changes, and the disappearance of the positive fingerprint band at 1190 cm^{-1}, indicative of deprotonation of the Schiff base; Hessling et al., 1993; Uhmann et al., 1991; Zscherp and Heberle, 1997). Because the spectral intensity at this position is still negative in the last spectrum, the N state has not yet appeared to an extent influencing the evaluation (Hessling et al., 1993; Pfefferlé et al., 1991; Zscherp and Heberle, 1997). The data presented in Fig. 1, *A* and *B*, will be used further, as decribed in the strategy section.

Application of procedure I

For the analysis of the spectra we used a unidirectional reaction model (Chizhov et al., 1996). For this, we first applied a global fit to the slow data set as described in Materials and Methods. The resulting time constants ($1/k$) are 0.78 (τ1), 2.7 (τ2), 40 (τ3), 134 (τ4), 544 (τ5) μs, and 1.6 (τ6), 5 (τ7), and 9.6 (τ8) ms (Table 1). The first time constant has been confirmed by fitting the fast data set. The

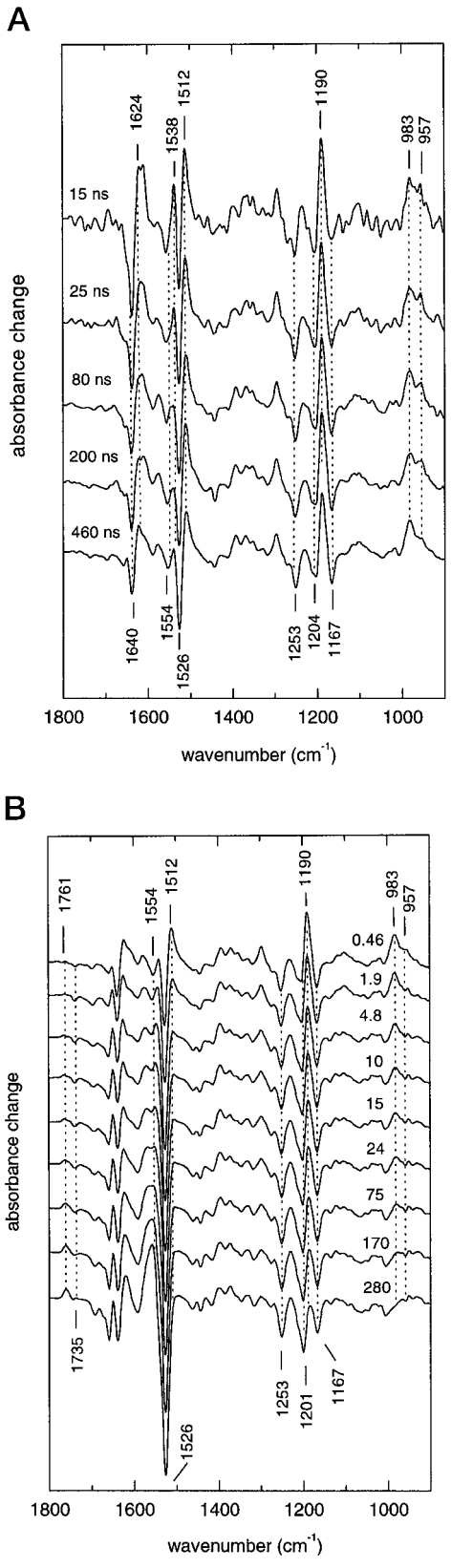

FIGURE 1 (*A*) Time-resolved FTIR difference spectra of the BR photoreaction at pH 7 and 298 K at 15, 25, 80, 200, and 460 ns after photolysis. The spectra were normalized to equal amounts of BR ground state at 1253 cm^{-1} to compensate for the instrumental rise time. (*B*) Time-resolved FTIR difference spectra of the BR photoreaction at pH 7 and 298 K in the time range 0.46–280 μs after photolysis.

TABLE 1 Apparent time constants of the BR photocycle at different pH values

pH	τ1 (μs)	τ2 (μs)	τ3 (μs)	τ4 (μs)	τ5 (μs)	τ6 (ms)	τ7 (ms)	τ8 (ms)
5.3	0.81	—	24	67	347	1.4	3.8	—
7	0.78	2.7	40	134	544	1.6	5.0	9.6
8	0.88	—	19.8	83	998	1.5	5.9	13.6
9.5	—	0.95	7.8	113	1800	(6.5)*	(12.4)*	—
No buffer	0.9	3	38	105	531	(8.9)*	—	—

*Values may be distorted by incomplete data acquisition.

values are in good agreement with the recent analysis of time-resolved UV-vis data by one of us (Chizhov et al., 1996). The corresponding amplitude spectra are shown in Fig. 2. We realized that the microsecond time range cannot be easily fitted to a reaction model involving only pure intermediates, which further justifies the adopted methodology. From these amplitude spectra and corresponding time constants, the difference spectra for the equilibria are obtained. The results are shown in Fig. 3 *A*. For clarity, it should be mentioned that although in Fig. 3 *A* intermediate spectra are labeled with their decay time constants, in the following a spectrum is sometimes named by its rise time, which, of course, is identical to the decay time of the preceeding intermediate.

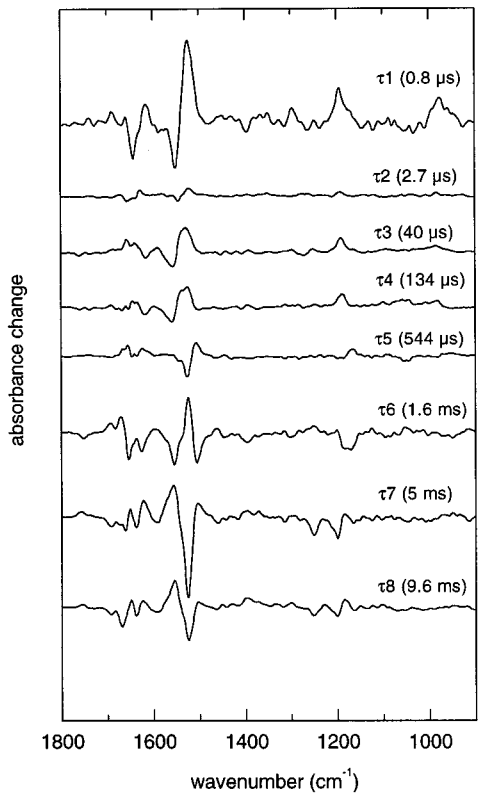

FIGURE 2 Amplitude spectra obtained by a global multiexponential fit of the BR photoreaction at pH 7 and 298 K with eight exponentials in the time range of 1.4 μs to 160 ms. The corresponding time constants are given in parentheses.

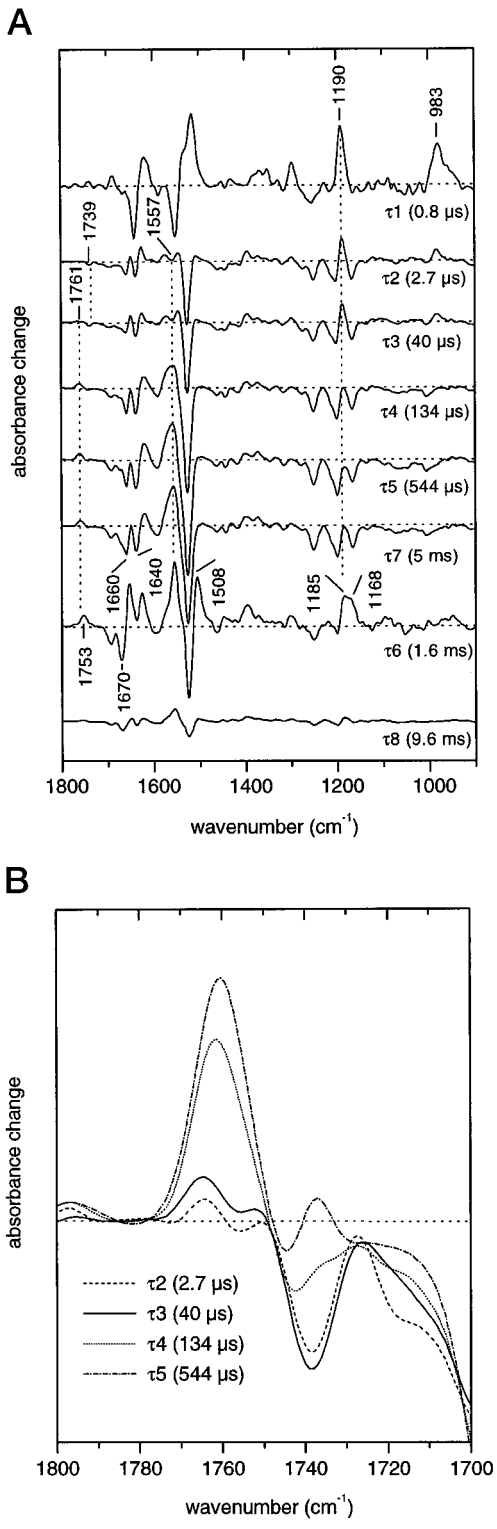

FIGURE 3 (*A*) Intermediate spectra of the BR photocycle at pH 7, calculated from the amplitudes and time constants shown in Fig. 2 by applying a linear sequential reaction model. Horizontal dotted lines indicate the zero line of each spectrum. The decay time constants of the intermediates are given in parentheses. (*B*) Expanded region of carboxyl groups of spectra corresponding to $\tau 2$, $\tau 3$, $\tau 4$, $\tau 5$ in *A*. The horizontal dotted line indicates the zero line of the spectra. The decay time constants of the intermediates are given in parentheses.

The first spectrum essentially corresponds to the late KL spectrum of Fig. 1 *A*, although it is somewhat distorted by the increased response time. The next spectrum has all of the characteristics of the L state. It is important to mention that this spectrum still contains a clear HOOP mode at 983 cm^{-1}. The lack of a clear ethylenic mode at lower frequencies shows that little if any KL contributes to the spectrum, i.e., the KL $\rightarrow$ L transition is essentially unidirectional. Therefore, the HOOP mode cannot be explained by the presence of KL. Changes between the third and second spectra are very small, and they can only be clearly identified by subtraction (see below). However, the small absorbance increase at 1761 cm^{-1} (Fig. 3 *B*) and the reduced size of the band at 1190 cm^{-1} indicate that to a small extent the Schiff base is already deprotonated and Asp^{85} is protonated, i.e., the spectrum is characterized by an L/M equilibrium with little M contribution. In the transition with a time constant of 40 μs, the major part of M is already present, but the somewhat positive absorbance at 1185 cm^{-1} indicates that a small amount of L still contributes. (Because of the overlap with the negative bands of the BR state, the maximum absorbance shifts from 1190 cm^{-1} to 1185 cm^{-1} during L decay.) Thus this spectrum corresponds to an L/M equilibrium favoring the M state. It is only with the time constant of 134 μs that an almost pure M state is generated. The main evidence for this is the negative absorbance at 1185 cm^{-1}, the smaller intensity of the band at 1660 cm^{-1} as compared to the band at 1640 cm^{-1} (Hessling et al., 1993; Zscherp and Heberle, 1997), and the reduction in absorbance at 983 cm^{-1}. However, the comparison of this spectrum with the $\tau 5$ spectrum at pH 9.5 (Fig. 9) shows a somewhat larger negative absorbance in the latter. Therefore, the intermediate at pH 7 cannot be pure M. Comparison with spectrum $\tau 7$ shows that the spectral features typical of N have not yet developed (see the discussion of the $\tau 7$ spectrum below), in agreement with previous time-resolved studies (Váró and Lanyi, 1991b). Therefore, we attribute this admixture to L. This L contribution does not interfere with the calculation of the L/M difference spectra, because these spectra are normalized to equal amounts of L.

Although the later transitions are not of relevance for the detection of early and late M states, the spectra will be briefly described. We applied the submodel B of Chizhov et al. (1996), i.e., the order of $\tau 6$ and $\tau 7$ was reversed. The following spectrum (rise with 544 μs) shows contributions from N (rise of intensities of the negative band at 1670 cm^{-1} and of the positive band at 1557 cm^{-1}, as well as the increase in absorbance at 1185 cm^{-1}). Thus the spectrum represents an M/N mixture in which the equilibrium is on the side of M. The next spectrum corresponds to a mixture of N and O (ethylenic mode at 1508 cm^{-1}, fingerprint bands at 1185 and 1168 cm^{-1}; Zscherp and Heberle, 1997). The lack of absorbance around 1761 cm^{-1} indicates little contribution from M. The small size of the bands in the last spectrum demonstrates that there must be a mixture between an intermediate and the ground state. With the exception of

this last spectrum, the other results coincide with the analysis of the UV-vis data (Chizhov et al., 1996).

The three time constants for the L → M transition have been interpreted as describing transitions to three sequential L/M equilibria with increasing M content. The reason for not applying a model with parallel L-to-M transitions from three populations with structurally different BR populations, which also would be an adequate description of the observed time constants, is related to the later part of the photocycle. Here the adopted model describes well the N/O and M/N equilibria detected by temperature jump (Chernavskii et al., 1989) and double pulse excitation experiments (Druckmann et al., 1993), whereas these experiments would be difficult to explain with a model involving parallel photocycles from different BR populations. Therefore we regard a model with parallel L → M transitions as rather unlikely.

To unravel putative differences in the M states in the early and late L/M equilibria, the BR → L spectrum is subtracted from the spectra of the equilibria without normalization. The results for the spectra with decay times of 134 and 544 μs are shown in Fig. 4 (*upper part*). The first spectrum (*solid line*) is normalized to the second one (*dashed line*) by adjusting to equal intensity of the band at 1190 cm^{-1}. The normalization constant is 1.35. Thus 74% of M are present. The relative L and M contents in the two intermediate spectra are in good agreement with the corresponding analysis of time-resolved UV-vis spectra (Chizhov et al., 1996). Because the band at 1761 cm^{-1} has the same amplitude in the two spectra (protonation of Asp^{85} by the Schiff base), the normalization factor is confirmed. The large negative band around 1530 cm^{-1} contains contributions from the ethylenic modes of L and from amide II spectral changes. Small but significant differences between the two spectra can be seen at 1557 and 1616 cm^{-1}. In the first spectrum the two bands have lower intensities. It is important to note that these differences do not arise from N contributions, because no bands characteristic of N are observed. This confirms our assumption that the intermediate τ5 (Fig. 3 *A*) is free from N contaminations. For the spectrum with a decay time of 40 μs, a normalization factor of 6.8 was obtained, indicating that only 15% of M are present. This large normalization factor causes excessive noise in the corresponding spectrum, which is therefore omitted from Fig. 4. Nevertheless, within the limits imposed by the noise, two observations are noteworthy: 1) The band due to protonation of Asp^{85} has the same intensity and position as in the other two spectra. 2) The intensity of the bands at 1557 and 1616 cm^{-1} appears to be drastically reduced. In addition, the presence of M in the intermediate spectrum with a decay time of 40 μs is directly indicated by an absorbance increase at 1761 (Fig. 3 *B*) and a decrease in the band intensity at 1190 cm^{-1} (Fig. 3 *A*).

To confirm these tendencies, we applied the second strategy to the analysis of the spectra in Fig. 1 *B*. The idea is that in the time range of 10–40 μs, this spectral difference in the early L → M spectra may be more easily detected, because the noise is reduced, although the size of the intensity difference between the two bands may be reduced.

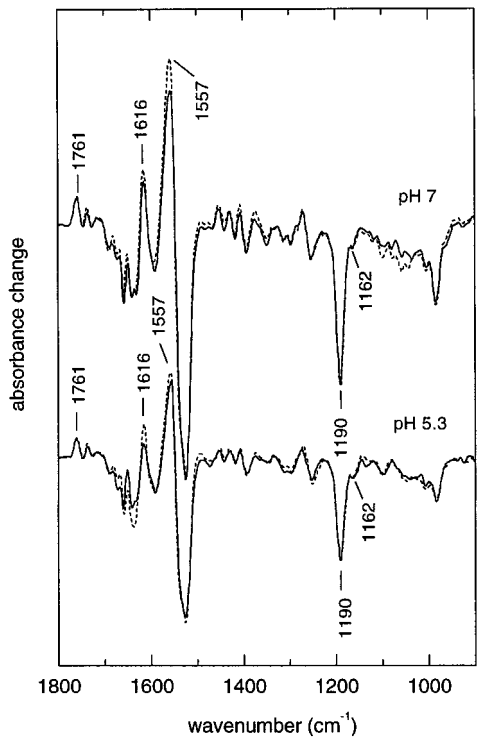

FIGURE 4 Calculated L → M difference spectra at pH 7 (*top*) and pH 5.3 (*bottom*). The spectra at pH 7 are obtained by subtracting the L-intermediate spectrum τ2 in Fig. 3 *A* from the M-intermediate spectra τ4 and τ5 in Fig. 3 *A*. The resulting spectra were normalized to equal band intensity at 1190 cm^{-1}. The same procedure was applied to the intermediates τ3, τ4, and τ5 at pH 5.3 shown in Fig. 8. ——, Subtraction from spectra τ4; – – –, subtraction from spectra τ5.

Application of procedure II

As mentioned in the Strategy section, the early spectra of Fig. 1 *B* have to be corrected for KL contributions. To avoid any systematic errors by applying an inadequate reaction model, we empirically determined the amount of KL in the spectra by using a characteristic band of the KL state. The band at 1512 cm^{-1} (ethylenic stretch of the chromophore in KL) seems to represent a good indicator. However, because this band is distorted by overlap with the strong negative band of the corresponding vibration of the ground state and by amide II spectral changes, the subtraction constant cannot be unequivocally determined. Another feature of the KL state is the HOOP mode around 957 cm^{-1} (Fig. 1, *A* and *B*). This band appears to be influenced by the overlap with a difference band located at approximately the same position, which is present with equal intensity in all of the spectra of Fig. 1 *B* (HOOP mode in the L and M states). Therefore, to clearly determine the contribution of the broader HOOP mode of KL in the spectra of Fig. 1 *B*, we subtracted the last one (280 μs) from all of the others, thereby essentially

forming $M_{late} \rightarrow KL/L/M_{early}$ difference spectra. Thus the common HOOP mode of the chromophore in L and M is canceled. The result for the first four spectra of Fig. 1 *B* is shown in Fig. 5.

The positive band at 1190 cm^{-1} represents the C_{11}-C_{12} stretching vibration of the KL and L states (Gerwert and Siebert, 1986), and the band at 983 cm^{-1} the 15-HOOP mode of both states (Weidlich and Siebert, 1993; Dioumaev and Braiman, 1997). Because the band at 959 cm^{-1} is now clearly visible, the contribution of the KL state to the spectra is much easier to determine. To also correct for very small contributions of the KL state, the spectra of Fig. 5 have been artificially normalized to equal amplitude of the band at 983 cm^{-1} (*inset A* of Fig. 5 for the corresponding spectral range). Now the band at 959 cm^{-1} can be easily quantified, and the spectra of Fig. 1 *B* can be corrected for the contribution of KL, resulting in the disappearance of the band at 959 cm^{-1} in the spectra of Fig. 5 (*inset B*). It turned out that only very little KL is present: 20% of KL has been subtracted from the 1.9-μs spectrum (mainly L), and 5% of KL has been subtracted from the 4.8-μs spectrum. For all of the other spectra the KL contribution was negligible. This is explained by the essentially unidirectional character of the KL $\rightarrow$ L transition mentioned above. After normalizing to equal amounts of BR, BR $\rightarrow$ L/M spectra are obtained from the spectra of Fig. 1 *B* with varying amounts of L and early and late M, which are not contaminated by contributions from KL (Fig. 6; only the first two spectra are corrected).

To identify spectral differences between early and late M states in the spectra of Figs. 6 and 1 *B*, the first spectrum (essentially representing the BR $\rightarrow$ L spectrum) is subtracted from all of the later spectra without further normalization, reflecting the temporal evolution after L formation (L $\rightarrow$ M spectra with varying amounts of early and late M). For a quantitative comparison, the spectra are normalized to equal amounts of L undergoing the transition to the M states. For this, the band at 1190 cm^{-1} representing the C_{11}—C_{12} stretching mode of the chromophore in L has been used (Gerwert and Siebert, 1986), and the normalization constants are 4, 2.6, 1.3, and 1 for the 10-, 24-, 170-, and 280-μs spectra, respectively (Fig. 7 *A*). Because of the decreasing normalization constant and the decreasing effective electronic bandwidth, the noise is continuously reduced from the first to the last spectrum. Taking these noise levels into account, there is overall good agreement among the spectra. The late spectra agree well with those of Fig. 4. It is important to mention that the 10-μs spectrum already represents a clear transition to the M state, because it shows a positive band around 1761 cm^{-1}, representing the proto-

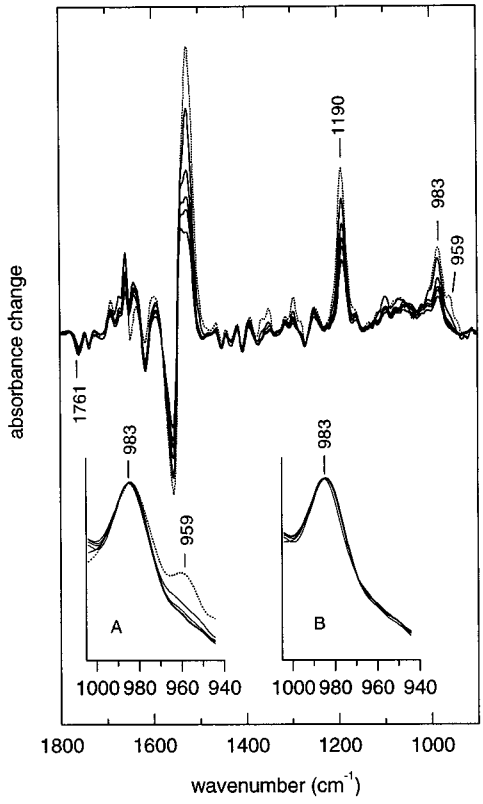

FIGURE 5 Determination of the KL contribution to the FTIR difference spectra in the early microsecond time range. Spectra resulting from subtraction of the late M spectrum at 280 μs (Fig. 2) from the spectra at 0.46, 1.9, 4.8, 10, and 15 μs (Fig. 2) are shown at the top. *Inset A*: The same spectra normalized to the HOOP band at 983 cm^{-1}. The KL-spectrum at 460 ns (·····) is subtracted 0.2 times from the 1.9-μs spectrum and 0.05 times from the 4.8-μs spectrum to cancel the KL-band around 959 cm^{-1} (*inset B*).

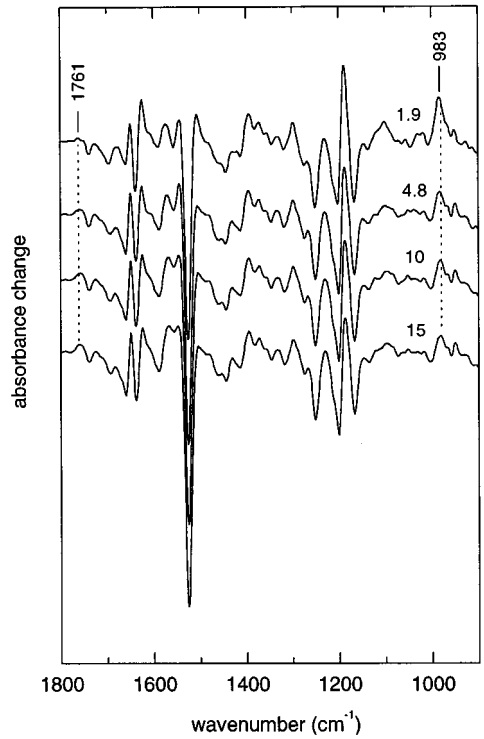

FIGURE 6 BR $\rightarrow$ L/M difference spectra at indicated times. The two top spectra (1.9 μs and 4.8 μs) are corrected for contributions from the KL intermediate (see Fig. 5) and renormalized to equal amounts of BR ground state.

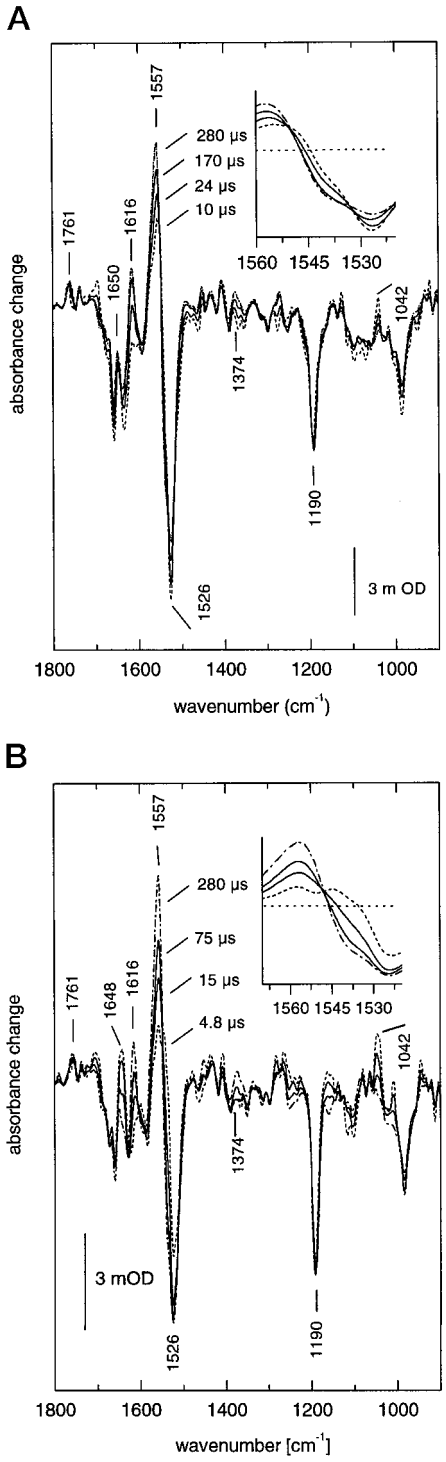

FIGURE 7 (*A*) Results of data evaluation according to procedure II for pH 7 data. L → M difference spectra at indicated times obtained by subtracting the corrected BR → L spectrum at 1.9 μs (Fig. 6) from the spectra at 10 μs (- - -), 24 μs, 170 μs, and 280 μs (– · –) (Fig. 2). The resulting spectra are normalized to equal intensity of the L-band at 1190 cm^{-1}. The expanded amide II range of these spectra is shown in the inset. (*B*) Results of data evaluation according to procedure II for data from unbuffered sample. L → M difference spectra at indicated times obtained by subtracting a corrected BR → L spectrum at 1.9 μs from the spectra at 4.8 μs (- - -), 15 μs, 75 μs, and 280 μs (– · –) (Fig. 2). The resulting spectra are normalized to equal intensity of the L-band at 1190 cm^{-1}. The expanded amide II range of these spectra is shown in the inset.

nation of Asp^{85} in M, and because the negative absorbance at 1190 cm^{-1} shows that the Schiff base is already deprotonated. From the normalization constant we can conclude that ~25% of the final M amplitude is already generated after 10 μs. In the 4.8-μs spectrum, the M amplitude is too small to allow a clear identification of this intermediate. Therefore,it is omitted. At a few positions in Fig. 7 *A*, there are clear deviations that increase with time (at 1616, 1557, and around 1545 cm^{-1}). The inset shows an enlarged view of the spectral range above 1525 cm^{-1}. The differences between the 280- and 170-μs spectra confirm the results deduced from the unidirectional reaction model. In addition, the 24- and 10-μs spectra clearly show that an additional M state must be present at earlier times with even further reduced band intensities at 1557 and 1616 cm^{-1}. This has already been tentatively concluded from the previous analysis. This M state is attributed to the very early L/M equilibrium with a decay time of 40 μs of Fig. 3 *A*. Thus combining the results from the two methods of analysis, it can be concluded that in the time range of 2–200 μs, three different M states can be identified. The first M state, appearing in ~3 μs, is characterized by very small band intensities at 1616, 1557, and 1545 cm^{-1}. In the second M state, with a rise time of ~40 μs, the two bands have almost but not yet completely attained the intensities of the final M state, which appears in 134 μs. It is not clear whether the spectral features represent a shift of an amide II band from 1545 cm^{-1} to 1557 cm^{-1} or intensity changes of two separate amide II bands. Therefore, a molecular interpretation is not possible at present. Almost identical results have been obtained for nonbuffered samples (Fig. 7 *B*) that were used to obtain additional data from samples at low salt concentration. Because of the very good signal-to-noise ratio, the 4.8 μs L/M difference spectrum could also be resolved.

Qualitatively, the increase in intensity at the three positions can already be deduced from the spectra in Fig. 1 *B*. However, it is not possible to directly discriminate between the rise of M and the transition between early and late M. The identification of an early M state in which these protein changes have not yet taken place has only been possible with the employed methods. Interestingly, both in early and late M, the band due to protonation of Asp^{85} is located at 1761 cm^{-1}.

It is important to comment here on the accuracy of the derived differences. As has been mentioned in the preceding paragraph, noise will mainly distort the spectra of the early time range. It will be especially large between 1660 and 1630 cm^{-1}, where the infrared transmission of the sample is very low because of amide I and water absorbance. This does not apply to the region between 1570 and 1530 cm^{-1} (amide II), because here water absorbance does not contribute and amide II absorbance is somewhat smaller than amide I absorbance. In Fig. 7, *A* and *B*, besides the differences discussed so far, additional smaller differences seem to be present. To decide whether these differences are due to noise, we repeated the measurements at pH 7 twice and

performed additional two measurements without buffer. From the analysis of these additional data (not shown), we could conclude that 1) the large spectral differences at 1616, 1557, and 1545 cm^{-1} are reproduced and 2) that the only additional real differences may be located at 1374 and 1042 cm^{-1}. All other spectral differences in Fig. 7, *A* and *B*, and especially those observed between 1660 and 1640 cm^{-1} are most probably caused by noise in the spectra.

In our opinion it is unlikely that the observed spectral differences can be attributed to different L states. Comparing the early L spectrum ($\tau 2$ in Fig. 3 *A*) with the late M spectrum ($\tau 5$ in Fig. 3 *A*), positive bands attributed to the M state are observed at positions around 1616 and 1557 cm^{-1} and a negative band at 1545 cm^{-1}, which has not yet developed in L. At these positions we obtain developing bands with a corresponding sign in the calculated L/M difference spectra (Figs. 4, 7 *A*, and 7 *B*). Assuming a single M intermediate, the corresponding bands should already be observed in the earliest M spectrum. Because this is not the case, alterations in the L state must compensate for these bands of the M state. Thus the spectral changes that take place in the transition between L states would have to be reverted in the transition to M. This appears to be highly unlikely.

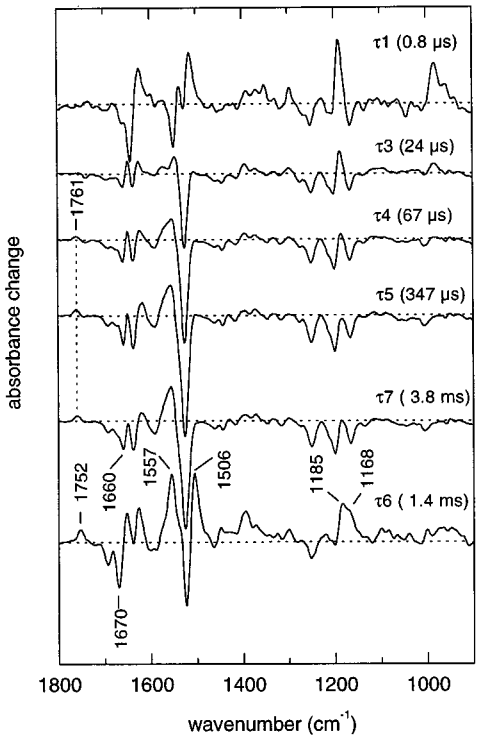

FIGURE 8 Intermediate difference spectra of the BR photoreaction at pH 5.3, calculated from the amplitudes and time constants from a global multiexponential fit with six exponentials in the time range of 1.4 μs to 160 ms by applying a linear sequential reaction model analogous to the procedure for pH 7 data (Fig. 3). Horizontal dotted lines indicate the zero line of each spectrum. The decay time constants of the intermediates are given in parentheses.

Measurements at other pH values

To obtain information on the functional role of the different M states, we performed corresponding measurements at pH 5.3, 8, and 9.5. For the pH 5.3 data, the difference spectra to the equilibria together with the corresponding decay times are shown in Fig. 8. Here, six exponentials were sufficient to fit the data. It is especially noteworthy that no time constant corresponding to that of 3 μs of the pH 7 or unbuffered measurements could be identified. This is probably due to the considerably reduced value of $\tau 3 = 24$ μs (pH 5.3) as compared to $\tau 3 = 40$ μs (pH 7) (Table 1). As in the corresponding spectra of Fig. 3 *A*, the first two spectra correspond to essentially pure KL and L states. The next spectrum (decay time 67 μs) consists of a mixture of L and M, because it still has some positive absorbance at 1185 and 983 cm^{-1} and a negative absorbance at 1740 cm^{-1} (characteristic features of L spectra), whereas the positive band at 1761 cm^{-1} (protonation of Asp^{85}) indicates a considerable contribution from M. In the spectrum with a decay time of 347 μs, the amount of L is reduced. As compared to the 544-μs spectrum of the pH 7 measurement (Fig. 3 *A*), the absorbance at 1185 cm^{-1} is less negative. Because the band due to Asp^{85} is still located at 1761 cm^{-1}, we assign this reduced negative absorbance to a small contribution from L but not from N, in which the band due to Asp^{85} is shifted down to 1755 cm^{-1} (Pfefferlé et al., 1991; Hessling et al., 1993; Zscherp and Heberle, 1997). The further observation that the late M state is equilibrium with L is in agreement with the analysis of time-resolved UV-vis investigations (Zimányi et al., 1992b) and resonance Raman investigations (Althaus and Stockburger, 1998). Neglecting the small contribution from Asp^{96} and Asp^{115} in the BR $\rightarrow$ M spectra (Sasaki et al. 1994), we used the negative band at 1740 cm^{-1} in L as a criterion for roughly estimating the amount of L in the early and late L/M equilibrium, which was determined to be 50% and 15%, respectively. Only in the next spectrum can some N be detected, because the Asp^{85} band is somewhat downshifted. As in the $\tau 6$ spectrum of Fig. 3 *A*, the last spectrum consists of a mixture of N and O, the O fraction being larger in Fig. 8 (relative band intensities 1185 versus 1168 cm^{-1} and 1557 versus 1506 cm^{-1}).

As for the pH 7 measurements, we formed the normalized L $\rightarrow$ M difference spectra, which are shown in the lower part of Fig. 4. It is obvious that the same small spectral differences are observed (the deviations in the extent of the spectral differences between the two measurements are within the noise limit). For the measurements at pH 8, the time constants given in Table 1 were obtained. As for the pH 5.3 measurement, $\tau 2$ is missing. Again, this can be explained by the considerably smaller value of $\tau 3$. But by applying the same procedure to these data as for the pH 5.3 measurement, identical spectral differences for the two late M states have been obtained (not shown). Therefore, with respect to the late M states, the measurements at pH 5.3 and 8 confirm the previous results.

It is known that at high pH the rise time of M is considerably shortened (Liu, 1990; Bitting et al., 1990; Balashov et al., 1991; Váró and Lanyi, 1990). It is of interest which of the M states is actually formed at early times. Therefore we performed step-scan measurements at pH 9.5 and subjected the spectra to analysis with the unidirectional reaction model. It has to be mentioned that because of the considerably prolonged cycling time we were not able to cover with the limited memory of our data acquisition system the total length of the photocycle. For the global fit, six exponentials plus a constant difference spectrum were necessary to reproduce the data. The corresponding time constants are 0.95, 7.8, and 113 μs, and 1.8, 6.5, and 12.4 ms (Table 1). Because of this incomplete description of the photocycle, the spectra obtained by the analysis may be distorted for the last two time constants, but the earlier spectra are not influenced by the curtailed data acquisition. Therefore, in Fig. 9 only the first four spectra of the anlysis are shown.

As for previous measurements, the first spectrum describes a rather pure KL state. However, the next one already has a large admixture of M, as indicated by the band at 1761 cm^{-1}. Therefore, within the framework of our data analysis, KL decays to an equilibrium of L and M. This shows that there must be a fast decay of L, which is characterized by a time constant approximately equal to or even faster than that of the KL decay. Therefore this time constant is labeled τ2 in Table 1. In the τ4 spectrum with a decay time of 113 μs, the amount of L is decreased, and the τ5 spectrum essentially represents a pure M spectrum. This can be verified by comparison with the τ4 spectrum of Fig. 3 *A*. From this we can estimate that the two L/M equilibria contain 62% and 90% of M, i.e., 62% of M already appears within 0.95 μs, in agreement with time-resolved UV-vis measurements. We first made an attempt to derive a BR $\rightarrow$ L spectrum by subtracting a suitable fraction of the τ4 spectrum from the τ2 spectrum. However, it turned out that, as compared to the previous L spectra, severe deviations appear around 1557 cm^{-1}. These deviations are caused by the different M states present in the two spectra. Therefore, no reliable L $\rightarrow$ M difference spectra can be calculated that could be used to unequivocally derive spectral differences between the early and late M states. However, the spectra in Fig. 9 show clearly that there are large changes around 1557 cm^{-1} that cannot be explained by varying amounts of L, because the band at 1761 cm^{-1} due to the protonation of Asp^{85} exibits a considerably smaller relative increase. Therefore, qualitatively we can conclude that also at pH 9.5 the various M states differ in the size of a band around 1557 cm^{-1}. Because no reliable L spectrum can be derived from the spectra of the two equilibria, considerable spectral differences must already be present between the first two M states. Therefore, the first equilibrium (decay time 7.8 μs) probably corresponds to the first equilibrium of the pH 7 measurements (decay time 40 μs).

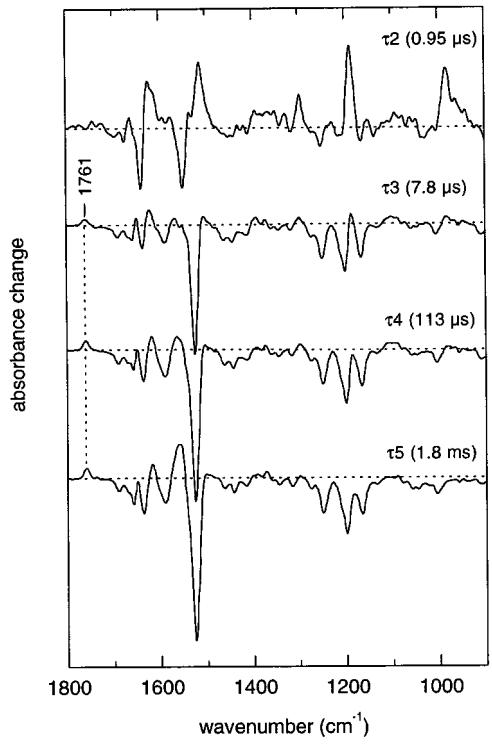

FIGURE 9 Intermediate difference spectra of the BR photoreaction at pH 9.5, calculated from the amplitudes and time constants from a global multiexponential fit with six exponentials in the time range of 1.4 μs to 160 ms by applying a linear sequential reaction model analogous to the results in Fig. 3. Horizontal dotted lines indicate the zero line of each spectrum. The decay time constants of the inermediates are given in parentheses. Only the first four intermediate spectra are shown.

DISCUSSION

First the results obtained for the 10–500-ns time range will be discussed in the framework of other published data. As already stated, the nanosecond spectra are in generally good agreement with recently published step-scan FTIR spectra (Hage et al., 1996; Dioumaev and Braiman, 1997). In particular, the decrease in the fingerprint mode around 1190 cm^{-1} and the decrease in the HOOP mode at 957 cm^{-1} in the time range from 100 to 500 ns indicate the presence of two KL states, as shown before in a careful kinetic analysis (Dioumaev and Braiman, 1997). Our data indicate an additional transition: the very early spectra are characterized by larger difference bands in the amide I range (1640 negative/1624 positive) and the amide II range (1554 negative/1538 positive), which decay within 30 ns (in Fig. 1 *A* only the 15-ns and 25-ns spectra are shown for this time range). In this respect it is interesting to note that we have obtained additional evidence for such a transition by comparing the yield of photoproduct formation, using a frequency-doubled Nd:YAG laser with a 6-ns pulse width versus a dye laser pulse (pumped by an XeCl excimer laser) of 20 ns. With equal pulse energy and wavelength, the yield obtained with the dye laser was larger by a factor of ~2, and from this observation we concluded that some molecular changes take place during these 20 ns, reducing the probability of photo-

back-reactions (Weidlich et al., 1995). The larger intensity of the negative band in the very early spectra can also be seen in the data of Dioumaev and Braiman (1997). But the very fast changes in the amide II spectral range have not been described before. The negative band at 1554 cm^{-1}, which has been detected in our earlier published spectra with lower time resolution (Weidlich and Siebert, 1993), is confirmed here for the late KL state. This band is not present in the late KL spectrum of another step-scan measurement (Dioumaev and Braiman, 1997), but it can clearly be seen in the measurements performed with an infrared monochromator (Sasaki et al., 1993). This last observation in particular shows that this band is not an artifact due to our step-scan method.

The 15-H HOOP mode at 983 cm^{-1} in the L state deserves some further discussion. In the low-temperature L spectrum such a band is completely lacking. The presence of this band, however, is in agreement with recent step-scan measurements (Dioumaev and Braiman, 1997). The infrared intensity of such HOOP modes has been correlated with twists of the chromophore around the C-C single bond close to the corresponding CH group (Fahmy et al., 1989, 1991). Therefore, we must conclude that in room-temperature L, the geometry of the chromophore in the neighborhood of the Schiff base differs from that observed at low temperature. In particular, the HOOP mode indicates that the strong twist around the C_{14}—C_{15} single bond present in the KL state (Weidlich and Siebert, 1993) has not fully relaxed. Resonance Raman investigations have shown that the chromophore structure in L is very similar to that in N (Lohrmann and Stockburger, 1992; Fodor et al., 1988a,b; Eisfeld et al., 1993). However, the function of the Schiff base in these two states is different: in L, it donates the proton to Asp^{85} on the extracellular side, whereas in N it accepts a proton from Asp^{96} on the cytosolic side, suggesting that both the accessibility and the pK_a must be different. Our investigations indicate a clear difference between the two intermediates. The HOOP mode at 983 cm^{-1} is not present in N (Weidlich and Siebert, 1993). Quantum chemical calculations have shown that a twist around the C_{14}—C_{15} single bond can lower the pK_a (Schulten and Tavan, 1978). Thus the presence of this HOOP mode in room-temperature L and its absence in N could indicate differences in both the pK_a and accessibility. (Recent studies have estimated a pK_a of 8.5 for the N state of the D96N mutant (Brown and Lanyi, 1996) and probably even higher in wild-type BR, whereas it is thought to be lower in L, to partially protonate Asp^{85} in the early L/M equilibrium (Váró and Lanyi, 1991b,c). A further comment has to be made with respect to the L band at 1162 cm^{-1} (Fig. 4). In our earlier investigations of chromophore bands in low-temperature L, we have identified a band at 1155 cm^{-1} as the C_{14}—C_{15} stretching vibration (Gerwert and Siebert, 1986). This band cannot be seen in the room-temperature L $\rightarrow$ M difference spectra. However, the band at 1162 cm^{-1} is in agreement with room-temperature resonance Raman spectra (Fodor et al., 1988b). Thus this shift confirms that the conformation of the chromophore is slightly different in low-temperature versus room-temperature L.

Our data (Figs. 4, 7, and 9) clearly demonstrate the existence of two M states in the 50–200-μs time range. They can be discriminated by small differences in the intensities of bands located at 1616 and 1557 cm^{-1}. In addition, the pH 9.5 and pH 7 measurements and the masurements without buffer show that an early M state exists in the 1–5-μs time range in which the band at 1557 cm^{-1} has very low intensity. The latter two measurements indicate that the band at 1616 cm^{-1} typical of the late M state also has very low intensity in this early M. With respect to the spectral range between 1500 and 1700 cm^{-1}, this M state, which has not been described before, is very similar to the L state. In the following transition to the intermediate M state, both bands have almost reached their final size, and in the last transition much smaller absorbance increases occur at these two positions. The corresponding bands are caused by changes in the amide I/II modes and reflect small geometrical changes in the protein backbone.

To which molecular events of the proton transfer steps are these protein changes linked? It is generally accepted that protonation of Asp^{85} initiates the proton release process, because in wild-type BR the time course of the release process approximately parallels that of the rise of M (Heberle and Dencher, 1992; Alexiev et al., 1995), and proton release has never been observed to be faster than M rise in modified systems. Furthermore, because the proton is ejected whereas Asp^{85} stays protonated, it cannot be the proton from the Schiff base/Asp^{85} that is ejected; an additional site must be the proton donor (Siebert et al., 1982). Recent evidence suggests that the release site involves the residues Glu^{204} and Glu^{194} (Balashov et al., 1995, 1996; Brown et al., 1995; Richter et al., 1996a,b; Dioumaev et al., 1998). Proton release to the extracellular surface occurs at pH 7.5 and 22°C with a single time constant of 63 μs, whereas under the same conditions time constants for M rise of 1.4, 44, and 149 μs have been deduced (Heberle and Dencher, 1992). The latter values are in good agreement with our pH 7 measurements. Therefore, it is clear that in the first M state (1–5-μs time range), for which the L/M equilibrium is strongly shifted to the side of L, the proton release has not yet taken place, and the connectivity of the Schiff base must be still toward Asp^{85}. Thus it appears that the proton transfer to the membrane surface is triggered by the intermediate M state. This has also been concluded from the temperature dependence of the release rate: below 10°C it adopts the rate of the rise of the intermediate M state, whereas at higher temparature it proceeds with its own kinetics, with an activation energy that is only approximately half (35 kJ/mol) of that of the three rate constants of M rise (~65 kJ/mol) (Heberle and Dencher, 1992; Alexiev et al., 1995). The release must be initiated by a pK_a change of the corresponding site, and it has been suggested that this change is caused by protonation of Asp^{85}. Evidence for this has been derived from the complex titration behavior of Asp^{85} and Glu^{204} in the dark state, in which the protonation

state of each group influences the pK_a of the other residue (Balashov et al., 1995, 1996; Richter et al., 1996a,b). The observation that proton release at low temperature follows the kinetic of the rise of the intermediate M state demonstrates that in the light reaction protonation of Asp^{85}, as it occurs in the first M state, is not sufficient to trigger proton release. Instead, additional conformational changes must take place, which themselves may be triggered by protonation of Asp^{85} or already by the isomerization of the chromophore. These conformational changes have been detected in our measurements, as indicated by changes in amide I/II bands at 1616, 1557, and 1545 cm^{-1}, respectively. Thus, applying a unidirectional reaction model, it appears that the conformational changes occurring with the formation of the intermediate L/M equilibrium with 74% M are sufficient to cause full proton release. Here it is important to mention that the two time constants of 40 and 134 μs could also be determined by individual fitting of the absorbance changes at 1557 cm^{-1} to exponentials (not shown), i.e., the amide II changes are tightly coupled to the rise of the M state and do not reflect the proton release step itself.

What could be the role of the final M rise occurring with 134 μs at pH 7? Because the two amide bands show small, additional intensity increases, the conformation of this late M state is slightly different. The structural difference is in line with the observation that the kinetic for formation of the BR state upon illumination of the M state with a blue flash is slightly faster if the intermediate M state is excited as compared to excitation of the late M state (Druckmann et al., 1992). Further evidence has been obtained from infrared investigations using the same double-flash methodology (Hessling et al., 1997). It could be shown that the BR state reached within 1 μs differs, depending on whether the intermediate M state or the late M state was excited. Because the C═N stretch of the protonated Schiff base of the BR state at 1640 cm^{-1} appears most affected, this has been interpreted in terms of difference in hydrogen bonding of this group with the environment and, therefore, as a change in connectivity between the intermdiate and late M states. Therefore, one could speculate that the structural difference identified by us represents the molecular switch. However, the assignment of the band at 1640 cm^{-1} to the C═N stretch of the protonated Schiff base is not unequivocal, because other bands that react sensitively to changes in hydrogen bonding do not appear to be influenced (NH-bending at 1350 cm^{-1} (Smith et al., 1987; Massig et al., 1982; Siebert and Mäntele, 1983) and the band at 1254 cm^{-1}). Therefore, the difference between the two BR states observed at 1640 cm^{-1} could also reflect a change in an amide I band. Therefore, the identification of a change in connectivity appears to be only tentative, also in view of the fact that for the formation of both BR states the proton is taken up from Asp^{85}. To our knowledge, the only determination of the connectivity in an M state has been demonstrated by recent electric measurements under an applied voltage across the membrane (Nagel et al., 1998). Unfortunately, no infrared investigations can yet be performed under these conditions.

Because of these arguments and because of the small size of the absorbance changes between the intermediate and late M, we assume that the connectivity of the Schiff base has not changed between these two M states. Thus the connectivity is still toward Asp^{85}, or it has already changed toward Asp^{96} in the intermediate state. However, because L is still in equilibrium with the intermediate M, one has to assume that this intermediate M actually consists of a mixture of two M states with different connectivities. Such an M state with fluctuating accessibilities has recently been suggested (Brown et al., 1998). The small structural changes occurring in the transition to the late M state may simply reflect the shift of the L/M equilibrium to complete M formation. However, because our data do not provide direct evidence for the connectivity of the Schiff base, we cannot completely exclude the possibility that the switch occurs between the intermdiate and late M states.

Are these interpretations of the pH 7 measurements in line with the results obtained at other pH values? At pH 5.3, the formation of the late M state is connected to the shift of the L/M equilibrium from 50% L to 15% L. This long-lasting L/M equilibrium has been explained by the fact that at such low pH Glu^{204} remains protonated, and therefore, the pK_a of Asp^{85} is decreased (Richter et al., 1996a; Dioumaev et al., 1998). Again, small increases in the amide bands at 1616 and 1557 cm^{-1} are observed, which are very similar to those observed at pH 7 (Fig. 4). This would indicate that the protein conformational state is not directly linked to the pK_a of Asp^{85}. However, it should be noted that the accuracy of the spectra does not allow us to completely exclude the possibility that the size of the absorbance differences at pH 5.3 is somewhat smaller, which would indicate such a relationship. With respect to the connectivity, the same arguments apply to the two M states as have been presented for the intermediate and final M states of the pH 7 measurement. If the switch has already taken place, it requires that both M states consist of mixtures of two M states of different accessibilities. (If the switch occurs between the two M states causing the very small amide changes, one has to assume that only the late M state consists of such a mixture.) As for the pH 7 measurement, the proton release would be triggered by the transition with time constant $\tau 3$. However, because the pH is below the pK_a of the release site, proton ejection is delayed to the end of the photocycle (Richter et al., 1996a). At pH 9.5 Glu^{204} is already deprotonated in the initial state (Dioumaev et al., 1998). This has been suggested to be the cause for the fast rise of the M state, because deprotonation of Glu^{204} causes the rise of the pK_a of Asp^{85}, thereby shifting the L/M equilibrium toward larger M amplitude. This is in line with our measurements, because the first L/M equilibrium already contains 62% M. Furthermore, our measurements indicate that in this early M state the amide modes have not yet developed or have developed only to a small extent. Thus the pK_a of Asp^{85} (regulating the L/M equilibrium) is

not necessarily reflected in the intensity of these amide bands. We have shown that considerable amide II changes take place in the next two transitions (7.8 and 113 μs), during which 90% and 100% of M appears. As for the pH 7 measurements, these conformational changes would be responsible for the triggering of the pK_a change of the release site and, possibly, for the switch. Because the normal release site is already deprotonated in the initial state, proton release would be delayed until the end of the photocycle, and it would occur directly from Asp^{85}. Evidence for this has been obtained from measurements of the pH dependence of the flash-induced electric current used to monitor the proton release process (Kono et al., 1993; Dickopf and Heyn, 1997). The respective component of the current decreases above pH 8, and the responsible pK_a is probably that of Glu^{204} in the initial state (Dickopf and Heyn, 1997). It should be mentioned that a conformational change of the protein regulating the pK_a of the release site has recently been suggested (Althaus and Stockburger, 1998).

Because our investigations have not determined the connectivity of the Schiff base, we are unable to discriminate between the various models for the proton pumping mechanism proposed recently (Haupts et al., 1997; Spudich and Lanyi, 1996; Brown et al., 1998). However, if in the late M state characterized by us the connectivity is still toward Asp^{85}, another M state responsible for the switch has to be postulated. A possible candidate would be the MN intermediate described for the $Asp^{96} \rightarrow Asn$ mutant (Sasaki et al., 1992). It accumulates under steady-state illumination at high pH and has a deprotonated Schiff base, but from the large amide bands observed in FTIR difference spectra, its conformation is similar to that of N. Recent x-ray scattering experiments in combination with FTIR investigation support the FTIR conclusion (Kamikubo et al., 1997; Sass et al., 1997, 1998), although in the last two publications the intermediate has not been termed MN. It has been proposed that because reprotonation of the Schiff base in this mutant is slow (Miller and Oesterhelt, 1990; Holz et al., 1989; Otto et al., 1989; Gerwert et al., 1989), this new intermediate can accumulate. A very similar intermediate with large amide bands has been described for the $Asp^{85} \rightarrow Asn$ mutant, although it has not been termed MN at that time (Fahmy et al., 1992). Also here, reprotonation of the Schiff base is delayed (Heberle et al., 1993). An intermediate similar to the MN species has been identified in wild-type BR in the presence of glucose (Vonck et al., 1994). It is possible that glucose also slows down reprotonation of the Schiff base. In the MN state of wild-type bacteriorhodopsin, the reprotonation step itself could be too fast to enable the detection of this intermediate. Therefore, the molecular changes observed for the MN state (or for equivalent intermediates in other mutants or modifications) could well represent the molecular switch. If this is correct, the molecular changes responsible for the switch can be studied by monitoring the changes occurring for the N intermediate. Because for the $Trp^{182} \rightarrow Phe$ mutant and for BR regenerated with 9-demethyl retinal, we described an early N intermediate in which the strong negative amide I mode at 1670 cm^{-1} has not yet fully developed, but in which the other characteristics of N (1650 and 1557 cm^{-1}) are fully present (Weidlich et al., 1995, 1996), it seems possible that the corresponding slightly altered molecular changes reflect the switch. However, as for all modified systems, this early N state may be a peculiarity of the modification. To what extent could the chromophore contribute to the switch by adopting a conformation favoring the accessibility to either Asp^{85} or Asp^{96}? As described above, we have identified a pronounced band at 983 cm^{-1} in the room temperature L state as the 15-HOOP mode, which is absent in the N state. This indicates that the C_{14}—C_{15} bond of the chromophore is more strongly twisted in L than in N, because infrared HOOP intensities have been correlated with chromophore twists around neighboring single bonds (Fahmy et al., 1989). This could contribute to both regulation of the accessibility of the Schiff base and the pK_a of the Schiff base in L and N (Schulten and Tavan, 1978).

Note

A preliminary short report on part of this work has been presented at the International Conference on Time-Resolved Vibrational Spectroscopy, 1997, in Oxford, England (*Laser Chemistry*, in press).

This work was supported by the Fonds der Chemischen Industrie (to FS).

REFERENCES

Alexiev, U., R. Mollaaghababa, P. Scherrer, H. G. Khorana, and M. P. Heyn. 1995. Rapid long-range proton diffusion along the surface of the purple membrane and delayed proton transfer into the bulk. *Proc. Natl. Acad. Sci. USA.* 92:372–376.

Althaus, T., and M. Stockburger. 1998. Time and pH dependence of the L-to-M transition in the photocycle of bacteriorhodopsin and its correlation with proton release. *Biochemistry.* 37:2807–2817.

Ames, J. B., and R. A. Mathies. 1990. The role of back-reactions and proton uptake during the N → O transition in bacteriorhodopsin's photocycle: a kinetic resonance Raman study. *Biochemistry.* 29: 7181–7190.

Austin, R. H., K. W. Beeson, S. S. Chan, P. G. Debrunner, R. Downing, L. Eisenstein, H. Frauenfelder, and T. M. Nordlund. 1976. Transient analyzer with logarithmic time base. *Rev. Sci. Instrum.* 47:445–447.

Balashov, S. P., R. Govindjee, and T. G. Ebrey. 1991. Red shift of the purple membrane absorption band and the deprotonation of tyrosine residues at high pH origin of the parallel photocycles of trans-bacteriorhodopsin. *Biophys. J.* 60:475–490.

Balashov, S. P., R. Govindjee, E. S. Imasheva, S. Misra, T. G. Ebrey, Y. Feng, R. K. Crouch, and D. R. Menick. 1995. The two pKa's of aspartate-85 and control of thermal isomerization and proton release in the arginine-82 to lysine mutant of bacteriorhodopsin. *Biochemistry.* 34:8820–8834.

Balashov, S. P., E. S. Imasheva, R. Govindjee, and T. G. Ebrey. 1996. Titration of aspartate-85 in bacteriorhodopsin: what it says about chromophore isomerization and proton release. *Biophys. J.* 70:473–481.

Bitting, H. C., D.-J. Jang, and M. A. El-Sayed. 1990. On the multiple cycles of bacteriorhodopsin at high pH. *Photochem. Photobiol.* 51: 593–598.

Braiman, M. S., A. K. Dioumaev, and J. R. Lewis. 1996. A large photolysis-induced pK_a of the chromophore counterion in bacteriorhodopsin:

implication for ion transport mechanisms of retinal proteins. *Biophys. J.* 70:939–947.

Brown, L. S., L. Bonet, R. Needleman, and J. K. Lanyi. 1993. Estimated acid dissociation constants of the Schiff base, Asp-85, and Arg-82 during the bacteriorhodopsin photocycle. *Biophys. J.* 65:124–130.

Brown, L. S., A. K. Dioumaev, R. Needleman, and J. K. Lanyi. 1998. Local access model for proton transfer in bacteriorhodopsin. *Biochemistry.* 37:3982–3993.

Brown, L. S., and J. K. Lanyi. 1996. Determination of the transiently lowered pKa of the retinal Schiff base during the photocycle of bacteriorhodopsin. *Proc. Natl. Acad. Sci. USA.* 93:1731–1734.

Brown, L. S., J. Sasaki, H. Kandori, A. Maeda, R. Needleman, and J. K. Lanyi. 1995. Glutamic acid 204 is the terminal proton release group at the extracellular surface of bacteriorhodopsin. *J. Biol. Chem.* 270: 27122–27126.

Cao, Y., L. S. Brown, J. Sasaki, A. Maeda, R. Needleman, and J. K. Lanyi. 1995. Relationship of proton release at the extracellular surface to deprotonation of the Schiff base in the bacteriorhodopsin photocycle. *Biophys. J.* 68:1518–1530.

Chernavskii, D. S., I. V. Chizhov, R. H. Lozier, T. M. Murina, A. M. Prokhorov, and B. V. Zubov. 1989. Kinetic model of bacteriorhodopsin photocycle: pathway from m state to bR. *Photochem. Photobiol.* 49: 649–653.

Chizhov, I. V., D. S. Chernavskii, M. Engelhard, K.-H. Müller, B. V. Zubov, and B. Hess. 1996. Spectrally silent transitions in the bacteriorhodopsin photocycle. *Biophys. J.* 71:2329–2345.

Dickopf, S., and M. P. Heyn. 1997. Evidence for the first phase of the reprotonation switch of bacteriorhodopsin from time-resolved photovoltage and flash photolysis experiments on the photoreversal of the M-intermediate. *Biophys. J.* 73:3171–3181.

Dioumaev, A. K., and M. S. Braiman. 1997. Two bathointermediates of the bacteriorhodopsin photocycle, distinguished by nanosecond time-resolved FTIR spectroscopy at room temperature. *J. Phys. Chem. B.* 101:1655–1662.

Dioumaev, A. K., H. T. Richter, L. S. Brown, M. Tanio, S. Tuzi, H. Saito, Y. Kimura, R. Needleman, and J. K. Lanyi. 1998. Existence of a proton transfer chain in bacteriorhodopsin: participation of Glu-194 in the release of protons to the extracellular surface. *Biochemistry.* 37: 2496–2506.

Druckmann, S., N. Friedman, J. K. Lanyi, R. Needleman, M. Ottolenghi, and M. Sheves. 1992. The back photoreaction of the M intermediate in the photocycle of bacteriorhodopsin: mechanism and evidence for two M species. *Photochem. Photobiol.* 56:1041–1047.

Druckmann, S., M. P. Heyn, J. K. Lanyi, M. Ottolenghi, and L. Zimanyi. 1993. Thermal equilibration between the M and N intermediates in the photocycle of bacteriorhodopsin. *Biophys. J.* 65:1231–1234.

Ebrey, T. G. 1993. Thermodynamics of Membranes, Receptors and Channels. M. Jackson, editor. CRC Press, Boca Raton, FL. 353–387.

Eisfeld, W., C. Pusch, R. Diller, R. Lohrmann, and M. Stockburger. 1993. Resonance Raman and optical transient studies on the proton pump of bacteriorhodopsin reveal parallel photocycles. *Biochemistry.* 32: 7196–7215.

Fahmy, K., M. F. Grossjean, F. Siebert, and P. Tavan. 1989. The photoisomerization in bacteriorhodopsin studied by FTIR linear dichroism and photoselection experiments combined with quantum chemical theoretical analysis. *J. Mol. Struct.* 214:257–288.

Fahmy, K., F. Siebert, and P. Tavan. 1991. Structural investigation of bacteriorhodopsin and some of its photoproducts by polarized Fourier transform infrared spectroscopic methods—difference spectroscopy and photoselection. *Biophys. J.* 60:989–1001.

Fahmy, K., O. Weidlich, M. Engelhard, J. Tittor, D. Oesterhelt, and F. Siebert. 1992. Identification of the proton acceptor of Schiff base deprotonation in bacteriorhodopsin: an FTIR study of the mutant $Asp^{85} \rightarrow$ Glu in its natural lipid environment. *Photochem. Photobiol.* 56: 1073–1083.

Fodor, S. P. A., J. B. Ames, R. Gebhard, E. M. M. Van den Berg, W. Stoeckenius, J. Lugtenburg, and R. A. Mathies. 1988a. Chromophore structure in bacteriorhodopsin's N intermediate: implications for the proton-pumping mechanism. *Biochemistry.* 27:7097–7101.

Fodor, S. P. A., W. T. Pollard, R. Gebhard, E. M. M. Van den Berg, J. Lugtenburg, and R. A. Mathies. 1988b. Bacteriorhodopsin's L550 intermediate contains a C14–C15 s-trans-retinal chromophore. *Proc. Natl. Acad. Sci. USA.* 85:2156–2160.

Friedman, N., Y. Gat, M. Sheves, and M. Ottolenghi. 1994. On the heterogeneity of the M population in the photocycle of bacteriorhodopsin. *Biochemistry.* 33:14758–14767.

Gerwert, K., B. Hess, J. Soppa, and D. Oesterhelt. 1989. Role of aspartate-96 in proton translocation by bacteriorhodopsin. *Proc. Natl. Acad. Sci. USA.* 86:4943–4947.

Gerwert, K., and F. Siebert. 1986. Evidence for light-induced 13-*cis*, 14-s-*cis* isomerization in bacteriorhodopsin obtained by FTIR difference spectroscopy using isotopically labelled retinals. *EMBO J.* 5:805–811.

Hage, W., M. Kim, H. Frei, and R. A. Mathies. 1996. Protein dynamics in the bacteriorhodopsin photocycle: a nanosecond step-scan FTIR investigation of the KL to L transition. *J. Phys. Chem.* 100:16026–16033.

Haupts, U., J. Tittor, E. Bamberg, and D. Oesterhelt. 1997. General concept for ion translocation by halobacterial retinal proteins—the isomerization/switch/transfer (IST) model. *Biochemistry.* 36:2–7.

Heberle, J., and N. A. Dencher. 1992. Surface-bound optical probes monitor proton translocation and surface potential changes during the bacteriorhodopsin photocycle. *Proc. Natl. Acad. Sci. USA.* 89:5996–6000.

Heberle, J., D. Oesterhelt, and N. A. Dencher. 1993. Decoupling of photo- and proton cycle in the $Asp^{85} \rightarrow$ Glu mutant of bacteriorhodopsin. *EMBO J.* 12:3721–3727.

Hessling, B., J. Herbst, R. Rammelsberg, and K. Gerwert. 1997. Fourier transform infrared double-flash experiments resolve bacteriorhodopsin's M1 to M2 transition. *Biophys. J.* 73:2071–2080.

Hessling, B., G. Souvignier, and K. Gerwert. 1993. A model-independent approach to assigning bacteriorhodopsin's intramolecular reactions to photocycle intermediates. *Biophys. J.* 65:1929–1941.

Holz, M., L. A. Drachev, T. Mogi, H. Otto, A. D. Kaulen, M. P. Heyn, V. P. Skulachev, and H. G. Khorana. 1989. Replacement of aspartic acid-96 by asparagine in bacteriorhodopsin slows both the decay of the M intermediate and the associated proton movement. *Proc. Natl. Acad. Sci. USA.* 86:2167–2171.

Honig, B. H. 1978. Kinetic and molecular models for proton transport in bacteriorhodopsin. *In* Energetics and Structure of Halophilic Microorganisms. S. R. Caplan and M. Ginzburg, editors. Elsevier/North-Holland Biomedical Press, Amsterdam. 109–121.

Kamikubo, H., T. Oka, Y. Imamoto, F. Tokunaga, J. K. Lanyi, and M. Kataoka. 1997. The last phase of the reprotonation switch in bacteriorhodopsin: the transition between the M-type and the N-type protein conformations depends on hydration. *Biochemistry.* 36: 12282–12287.

Kataoka, M., H. Kamikubo, F. Tokunaga, L. S. Brown, Y. Yamazaki, A. Maeda, M. Sheves, R. Needleman, and J. K. Lanyi. 1994. Energy coupling in an ion pump. The reprotonation switch of bacteriorhodopsin. *J. Mol. Biol.* 243:621–638.

Kono, M., S. Misra, and T. G. Ebrey. 1993. pH dependence of light-induced proton release by bacteriorhodopsin. *FEBS Lett.* 331:31–34.

Lanyi, J. K. 1993. Proton translocation mechanism and energetics in the light-driven pump bacteriorhodopsin. *Biochim. Biophys. Acta.* 1183: 241–261.

Liu, S. Y. 1990. Light-induced currents from oriented purple membrane. I. Correlation of the microsecond component (B2) with the L $\rightarrow$ M photocycle transition. *Biophys. J.* 57:943–950.

Lohrmann, R., and M. Stockburger. 1992. Time-resolved resonance Raman studies of bacteriorhodopsin and its intermediates K590 and L550: biological implications. *J. Raman Spectrosc.* 23:575–583.

Massig, G., M. Stockburger, W. Gärtner, D. Oesterhelt, and P. Towner. 1982. Structural conclusion on the Schiff base group of retinylidene chromophores in bacteriorhodopsin from characteristic vibrational bands in the resonance Raman spectra of BR_{570} (all-*trans*), BR_{603} (3-dehydroretinal) and BR_{548} (13-*cis*). *J. Raman Spectrosc.* 12:287–294.

Mathies, R. A., S. W. Lin, J. B. Ames, and W. T. Pollard. 1991. From femtoseconds to biology: mechanism of bacteriorhodopsin's light-driven proton pump. *Annu. Rev. Biophys. Biophys. Chem.* 20:491–518.

Miller, A., and D. Oesterhelt. 1990. Kinetic optimization of bacteriorhodopsin by aspartate 96 as an internal proton donor. *Biochim. Biophys. Acta.* 1020:57–64.

Misra, S., R. Govindjee, T. G. Ebrey, N. Chen, J.-X. Ma, and R. K. Crouch. 1997. Proton uptake and release are rate-limiting steps in the photocycle of the bacteriorhodopsin mutant E204Q. *Biochemistry.* 36:4875–4883.

Müller, K.-H., and T. Plesser. 1991. Variance reduction by simultaneous multi-exponential analysis of data sets from different experiments. *Eur. Biophys. J.* 19:231–240.

Nagel, G., B. Kelety, B. Möckel, G. Büldt, and E. Bamberg. 1998. Voltage dependence of proton pumping by bacteriorhodopsin is regulated by voltage-sensitive ratio of M1 to M2. *Biophys. J.* 74:403–412.

Oesterhelt, D., J. Tittor, and E. Bamberg. 1992. A unifying concept for ion translocation by retinal proteins. *J. Bioenerg. Biomembr.* 24:181–191.

Otto, H., T. Marti, M. Holz, T. Mogi, M. Lindau, H. G. Khorana, and M. P. Heyn. 1989. Aspartic acid-96 is the internal proton donor in the reprotonation of the Schiff base of bacteriorhodopsin. *Proc. Natl. Acad. Sci. USA.* 86:9228–9232.

Pfefferlé, J. M., A. Maeda, J. Sasaki, and T. Yoshizawa. 1991. Fourier transform infrared study of the N intermediate of bacteriorhodopsin. *Biochemistry.* 30:6548–6556.

Rammelsberg, R., G. Huhn, M. Lübben, and K. Gerwert. 1998. Bacteriorhodopsin′s intramolecular proton-release pathway consists of a hydrogen-bonded network. *Biochemistry.* 37:5001–5009.

Richter, H. T., L. S. Brown, R. Needleman, and J. K. Lanyi. 1996a. A linkage of the pKa's of Asp-85 and Glu-204 forms part of the reprotonation switch in bacteriorhodopsin. *Biochemistry.* 35:4054–4062.

Richter, H. T., R. Needleman, and J. K. Lanyi. 1996b. Perturbed interaction between residues 85 and 204 in Tyr-185 → Phe and Asp-85 → Glu bacteriorhodopsin. *Biophys. J.* 71:3392–3398.

Rödig, C., and F. Siebert. 1998. Improvements in signal acquisition and processing for time-resolved step-scan FT-IR spectroscopy. *In* Fourier Transform Spectroscopy Eleventh International Conference. J. A. de Haseth, editor. American Institute of Physics, Woodbury, NY. 388–391.

Rothschild, K. J. 1992. FTIR difference spectroscopy of bacteriorhodopsin: toward a molecular model. *J. Bioenerg. Biomembr.* 24:147–167.

Sasaki, J., J. K. Lanyi, R. Needleman, T. Yoshizawa, and A. Maeda. 1994. Complete identification of C═O stretching vibrational bands of protonated aspartic acid residues in the difference infrared spectra of M and N intermediates versus bacteriorhodopsin. *Biochemistry.* 33:3178–3184.

Sasaki, J., A. Maeda, C. Kato, and H. Hamaguchi. 1993. Time-resolved infrared spectral analysis of the KL-to-L conversion in the photocycle of bacteriorhodopsin. *Biochemistry.* 32:867–871.

Sasaki, J., Y. Shichida, J. K. Lanyi, and A. Maeda. 1992. Protein changes associated with reprotonation of the Schiff base in the photocycle of Asp^{96} → Asn bacteriorhodopsin: the MN intermediate with unprotonated Schiff base but N-like protein structure. *J. Biol. Chem.* 267: 20782–20786.

Sass, H. J., R. Gessenich, M. H. J. Koch, D. Oesterhelt, N. A. Dencher, G. Büldt, and G. Rapp. 1998. Evidence for charge-controlled conformational changes in the photocycle of bacteriorhodopsin. *Biophys. J.* 75: 399–405.

Sass, H. J., I. W. Schachowa, G. Rapp, M. H. J. Koch, D. Oesterhelt, N. A. Dencher, and G. Büldt. 1997. The tertiary structural changes in bacteriorhodopsin occur between M states: x-ray diffraction and Fourier transform infrared spectroscopy. *EMBO J.* 16:1484–1491.

Schulten, K., and P. Tavan. 1978. A mechanism for the light driven proton pump of *Halobacterium halobium. Nature.* 272:85–86.

Siebert, F., and W. Mäntele. 1983. Investigation of the primary photochemistry of bacteriorhodopsin by low-temperature Fourier-transform infrared spectroscopy. *Eur. J. Biochem.* 130:565–573.

Siebert, F., W. Mäntele, and W. Kreutz. 1982. Evidence for the protonation of two internal carboxyl groups during the photocycle of bacteriorhodopsin. *FEBS Lett.* 141:82–87.

Smith, S. O., M. S. Braiman, A. B. Meyers, J. A. Pardoen, J. M. L. Courtin, C. Winkel, J. Lugtenburg, and R. A. Mathies. 1987. Vibrational analysis of the all-*trans* retinal chromophore in light adapted bacteriorhodopsin. *J. Am. Chem. Soc.* 109:3108–3125.

Spudich, J. L., and J. K. Lanyi. 1996. Shuttling between two protein conformations: the common mechanism for sensory transduction and ion transport. *Curr. Opin. Cell Biol.* 8:452–457.

Tittor, J., U. Schweiger, D. Oesterhelt, and E. Bamberg. 1994. Inversion of proton translocation in bacteriorhodopsin mutants D85N, D85T, and D85,96N. *Biophys. J.* 67:1682–1690.

Uhmann, W., A. Becker, C. Taran, and F. Siebert. 1991. Time-resolved FT-IR absorption spectroscopy using a step-scan interferometer. *Appl. Spectrosc.* 45:390–397.

Váró, G., and J. K. Lanyi. 1990. Pathways of the rise and decay of the M photointermediate(s) of bacteriorhodopsin. *Biochemistry.* 29: 2241–2250.

Váró, G., and J. K. Lanyi. 1991a. Distortions in the photocycle of bacteriorhodopsin at moderate hydration. *Biophys. J.* 59:313–322.

Váró, G., and J. K. Lanyi. 1991b. Kinetic and spectroscopic evidence for an irreversible step between deprotonation and reprotonation of the Schiff base in the bacteriorhodopsin photocycle. *Biochemistry.* 30: 5008–5015.

Váró, G., and J. K. Lanyi. 1991c. Thermodynamics and energy coupling in the bacteriorhodopsin photocycle. *Biochemistry.* 30:5016–5022.

Váró, G., L. Zimányi, M. Chang, B. Ni, R. Needleman, and J. K. Lanyi. 1992. A residue substitution near the β-ionone ring of the retinal affects the M substates of bacteriorhodopsin. *Biophys. J.* 61:820–826.

Vonck, J., B.-G. Han, F. Burkhard, G. A. Perkins, and R. M. Glaeser. 1994. Two progressive substates of the M-intermediate can be identified in glucose-embedded, wild-type bacteriorhodopsin. *Biophys. J.* 67: 1173–1178.

Weidlich, O., N. Friedman, M. Sheves, and F. Siebert. 1995. The influence of the 9-methyl group of the retinal on the photocycle of bacteriorhodopsin studied by time-resolved rapid-scan and static low-temperature FT-IR difference spectroscopy. *Biochemistry.* 34:13502–13510.

Weidlich, O., B. Schalt, N. Friedman, M. Sheves, J. K. Lanyi, L. S. Brown, and F. Siebert. 1996. Steric interactions between the 9-methyl group of the retinal and tryptophan 182 controls 13-*cis* to all-*trans* reisomerization and proton uptake in the bacteriorhodopsin photocycle. *Biochemistry.* 35:10807–10814.

Weidlich, O., and F. Siebert. 1993. Time-resolved step-scan FT-IR investigations of the transition from KL to L in the bacteriorhodopsin photocycle: identification of chromophore twists by assigning hydrogen-out-of-plane (HOOP) bending vibrations. *Appl. Spectrosc.* 47: 1394–1400.

Zimányi, L., Y. Cao, M. Chang, B. Ni, R. Needleman, and J. K. Lanyi. 1992a. The two consecutive M substates in the photocycle of bacteriorhodopsin are affected specifically by the D85N and D96N residue replacements. *Photochem. Photobiol.* 56:1049–1055.

Zimányi, L., G. Váró, M. Chang, B. Ni, R. Needleman, and J. K. Lanyi. 1992b. Pathways of proton release in the bacteriorhodopsin photocycle. *Biochemistry.* 31:8535–8543.

Zscherp, C., and J. Heberle. 1997. Infrared difference spectra of the intermediates L, M, N, and O of the bacteriorhodopsin photoreaction obtained by time-resolved attenuated total reflection spectroscopy. *J. Phys. Chem. B.* 101:1042–10547.